Research Article

Saja A. Kadhim*, Awham M. Hameed, and Rashed T. Rasheed

Synthesis and study of magnesium complexes derived from polyacrylate and polyvinyl alcohol and their applications as superabsorbent polymers

https://doi.org/10.1515/jmbm-2022-0053
received December 06, 2021; accepted June 18, 2022

Abstract: Novel superabsorbent polymers (SAPs) were created by solution polymerization at ambient temperature using potassium polyacrylate (KPA), polyvinyl alcohol (PVA), and magnesium chloride as a cross-linking agent with different weights of 0.4, 0.5, 0.6, 0.7, 0.8, and 1 g for KPA and 0.33, 0.44, 0.55, 0.733, and 1.1 g for PVA. Fourier transforms infrared (FTIR) and UV-Vis spectroscopy were used to determine the chemical composition of the SAP complexes. The outcomes revealed that the KPA and PVA successfully interacted with the magnesium chloride. The morphology of the surfaces shows a uniform porous interconnected microstructure as revealed by field emission scanning electron microscopy. The effective preparation was confirmed by thermal characterization (thermogravimetric analysis and differential scanning calorimetry) of the SAPs. The influence of the cross-linker agent on the SAPs' water absorbency was examined. The magnesium polyacrylate (Mg-PA) (0.6 g of $MgCl_2$) SAP has a maximum swelling capacity of 650%, while that of magnesium polyvinyl alcohol (Mg-PVA) (0.55 g of $MgCl_2$) was 244%. The findings confirmed that the SAPs have excellent swelling and water-retaining capabilities. The strategy used in this investigation may function as a model for developing and widespread usage of SAPs in agriculture and horticulture.

Keywords: magnesium chloride, hydrogel, swelling ratio, water retention capacity

*** Corresponding author: Saja A. Kadhim,** Applied Sciences Department, University of Technology-Iraq, Baghdad, Iraq; Second Rusafa Education, Ministry of Education, Baghdad, Iraq, e-mail: as.18.49@grad.uotechnology.edu.iq
Awham M. Hameed, Rashed T. Rasheed: Applied Sciences Department, University of Technology-Iraq, Baghdad, Iraq

1 Introduction

A hydrogel represents a three-dimensional, interconnected synthetic polymer having a solid appearance that, thanks to hydrophilic polymers in its structure, could adsorb and retain a substantial amount of water. The gel is created by joining macromolecular chains, resulting in insoluble polymers [1–3]. The percentage of water absorbed by the gel when swelling is not less than 20% of the total gel weight. When the water absorption rate is greater than 95%, it is called a gel polymer with super water absorption [4,5]. Superabsorbent polymers (SAPs) are widely utilized in several applications, such as agriculture, sealing, coal dewatering, food additives [6,7], manufacture, tissue engineering and regenerative medicines [8,9], diagnostics [10], sewage treatment, drug-delivery systems, and cosmetics [11–13]. SAPs are classed as natural or synthetic polymers, depending on their source of origin. SAPs made from natural polymers like cellulose, chitosan (CS), and starch benefit from being biodegradable. However, their low water absorption rate must be employed in more significant quantities [14,15]. SAPs made from synthetic polymers, such as polyacrylic acid (PAA), polyacrylamide (PAM), and polyvinyl alcohol (PVA), on the other hand, have cheap costs, extended service lives, and a high water absorption rate [16,17]. Even though SAPs have been extensively explored, enhancing their qualities, improving the theory, and increasing the controllability of their structural attributes are still significant concerns.

In this research, SAPs have been synthesized using industrial polymeric materials such as potassium polyacrylate (KPA) and PVA. KPA is a neutral hydrogel and has a linear-chain structure. Due to its great qualities, such as biocompatibility, inertness, and non-toxicity, it is used for paints and cosmetics, emerging applications, drilling fluids, and metal quenching [18]. KPA has become a perfect backbone for the production of SAPs [19].

In addition, PVA is an artificial hydrophilic polymer with a medium water retention ability that is non-toxic and non-carcinogenic [20–23]. It is used to make paper, textile warp sizing, thickening, and various paints as beads or water solutions [24–26]. To meet the needs of agricultural applications, Elbarbary *et al.* used X-rays to create super-absorbent hydrogels made of polyacrylamide (PAAM) as well as Na-alginate (Alg) or CS [27]. PAA/PVA/yeast SAPs with interpenetrating polymer networks are used to form new SAPs [28]. Researchers utilized sawdust as a framework structure to prepare a SAP with acrylic acid (AA) and acrylamide (AM) [29]. Mechanical and thermal properties were greatly improved by PVA-based hydrogels with different loadings of microcrystal cellulose [30]. Other researchers in a separate investigation, solution polymerized carboxymethyl cellulose/acrylic acid (AA) and PVA-AA blends with benzoyl peroxide as an initiator to produce SAPs [31]. Czarnecka and Nowaczyk created SAPs from starch, AA, AM, PVA, 2-hydroxyethyl methacrylate, and 2-acrylamido-2-methylpropane sulfonic acid using the graft polymerization process [32]. Based on these hypotheses, we studied KPA and PVA by adding magnesium salt to form cross-linking. The SAP structures were described by Fourier transforms infrared (FTIR), UV-Vis spectroscopy, and scanning electron microscopy (SEM). In addition, the Thermogravimetric analysis (TGA) and Differential scanning calorimetry (DSC) described the thermal characterization of SAPs. Water absorption for SAP and water-retaining agents were studied.

2 Materials

In this study, it was used potassium polyacrylate $(C_3H_3KO_2)_n$ (99.9%, apparent density of 0.56 mL/g, monomer residual less than 500, potassium 21.60%, MAS Group Inc., China), PVA $(C_2H_4O)_n$ (the average molecular weight of 67,000 g/mol, degree of polymerization 1,400, ME Scientific Engineering Ltd, UK), magnesium chloride hexahydrate ($MgCl_2{\cdot}6H_2O$) (99.9%, Belgium), sodium hydroxide (NaOH) (99.9%; BDH Company).

3 Synthesis of SAPs

3.1 Preparation of magnesium polyacrylate (Mg-PA) SAPs

Figure 1 shows a stock solution of KPA (2.174% w/v) synthesized by dissolving 5 g KPA in distilled water

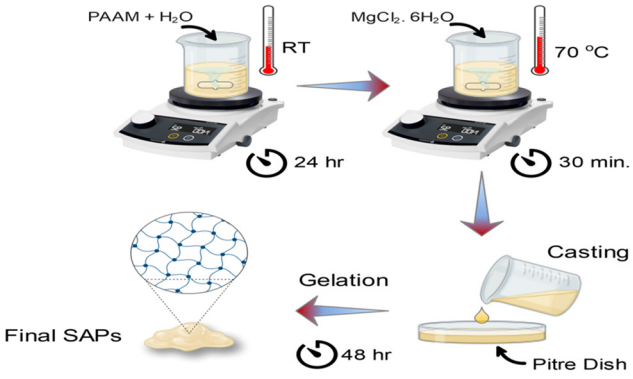

Figure 1: The preparation steps of Mg-KPA SAPs.

(230 mL). Weights of 0.4, 0.5, 0.6, 0.7, 0.8, and 1 g of $MgCl_2{\cdot}6H_2O$ were added separately to every 25 mL of stock solution and stirred using a magnetic stirrer for 30 min at 70°C. Execution of the reaction was done according to Figure 2. The precipitate was then collected after the water was removed and dried for a period of 48 h at 25°C.

3.2 Preparation of magnesium polyvinyl alcohol (Mg-PVA) SAPs

Figure 3 shows a synthesized PVA solution (2.174% w/v) by melting 5 g of polymer material in a basic solution (25 mL) with an 8:100 ratio of NaOH to distilled water. Weights of 0.33, 0.44, 0.55, 0.733, and 1.1 g of $MgCl_2{\cdot}6H_2O$ were separately added to the solution and stirred using a magnetic stirrer for 30 min at 70°C. The reaction took place according to Figure 4. Afterward, the prepared complex was emptied in a petri dish and then dried at 25°C for 48 h.

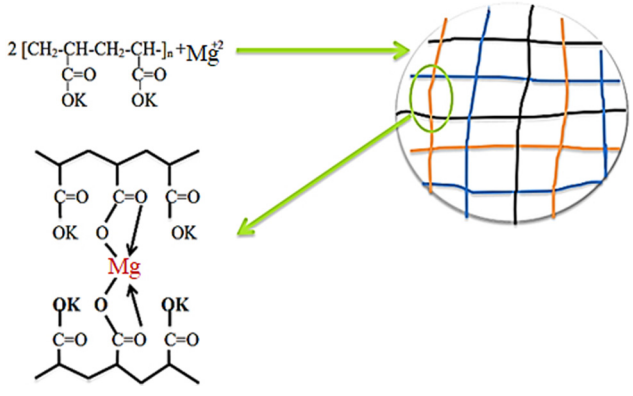

Figure 2: Mg-PA SAP reaction.

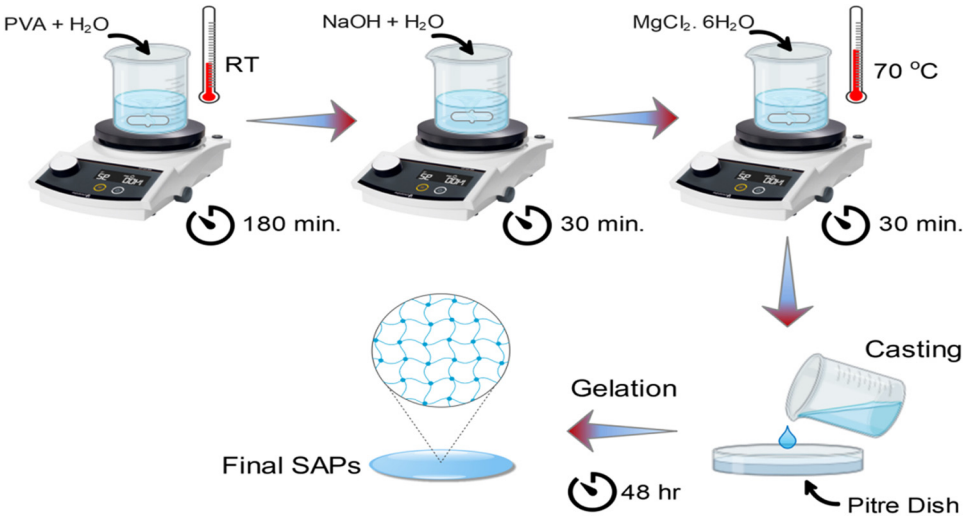

Figure 3: The preparation steps of Mg-PVA SAPs.

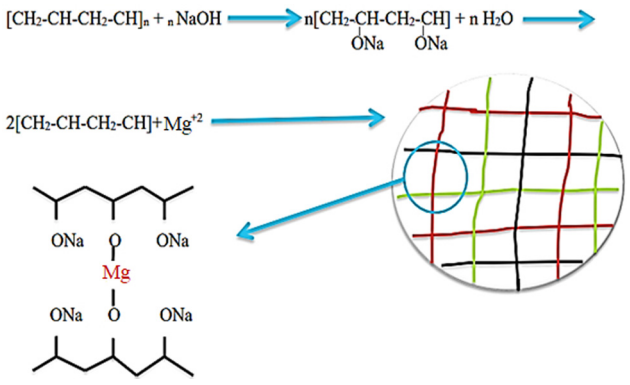

Figure 4: Mg-PVA SAP reaction.

4 Analytical methods

The SHIMADZU-8400S FTIR spectrometer from Japan was used to obtain Fourier converted infrared FTIR spectra. The spectra were obtained within the wavenumber range of 4,000–400 cm^{-1}. A TU-1901 spectrometer recorded the UV-Vis spectra (Purkinje General Instrument, China). SEM was used to test the morphological properties of SAPs using FESEM Zeiss sigma 300-HV, Germany with EHT = 5KV, and Mag = 100k×.

4.1 Swelling measurements of SAPs

Swelling kinetics refers to the time needed for Mg-PVA or Mg-PA complexes to reach their maximum swelling capacity. To carry out this experiment, different weights of dry complexes (Mg-PVA or Mg-PA) were used at different weights of salt (0.4, 0.5, 0.6, 0.7, 0.8, and 1 g) for KPA and (0.33, 0.44, 0.55, 0.733, and 1.1 g) for PVA. At 25°C, the complexes were sliced to small cuts, weighed, then immersed in distilled water for 24 h for the Mg-PA complex and for 9 h for the Mg-PVA complex. The swollen specimens were removed and weighed after being cleaned using filter papers to eliminate excess waters from the surface. Measuring each weight was done three times to get an average value. The following equation is used to calculate the degree of swelling [33]:

$$\text{Swelling Ratio (\%)} = [(W_S - W_D)/W_D] \times 100\%. \quad (1)$$

where W_S refers to the weight of wet specimens (g) after filtration and W_D is weight of the dried specimens (g).

4.2 Water retention of SAP

The SAPs water retention was examined utilizing the next procedure. By using distilled water, small pieces of SAPs were made to swell till saturation. At room temperature, SAPs were cleaned utilizing filter paper and then put in Petri plates. After a constant period, the weight of the SAPs was noted down. This process was repeated till the weight remained unchanged. The amount of water retention is calculated using the equation below [34]:

$$\text{Water retention capacity \%} = (W_T - W_D/W_S - W_D) \times 100\%. \quad (2)$$

where W_T denotes the weight of SAP at a time "T," W_D denotes the weight of dry SAP, and W_S indicates the weight of SAP when fully swelled.

4.3 Thermal studies

Underneath the nitrogen atmosphere, TGA was conducted with a Universal V4.5A (TA Instruments) at a temperature increment of 10°C/min in the range from 30 to 400°C. Underneath nitrogen atoms, different scattering calorimetry (DSC) was carried out using Universal V4.5A (TA Instruments) at a temperature increment of 10°C/min from 30 to 400°C.

5 Results and discussion

5.1 FTIR analyses of the samples

Figure 5 displays the FTIR absorption spectra of KPA and Mg-PA with 0.6 g of $MgCl_2.6H_2O$ SAP prepared by the solution polymerization technique. The broadband at 3,439 cm^{-1} is because of O–H stretching. The peaks at 2,924, 1,695, 1,602, 1,522, and 1,106 cm^{-1} can be ascribed to C–H stretch, carbonyl group (C═O) stretch, ν_{asym} (COO^-) stretch, C–H bending, and ν_{sym} (COO–) stretching of KPA, respectively [35–37].

The FTIR characteristic peaks of the Mg-PA spectrum (Figure 5) show a high wavenumber shift from 1,695 to 1,637 cm^{-1} ($\nu_{C=O}$ stretching) with a decreasing peak intensity. The downshift of this peak is due to the electrostatic attraction between the Mg^{2+} cation and the carbonyl group, which is a highly reactive group of KPA, and the downward shift from 1,602 to 1,599 cm^{-1} (ν_{asym} [COO^-]). This might be due to the strong interaction between the KPA's carboxyl group and magnesium. These results indicate that the carboxyl groups are act as bidentate ligands, this means magnesium chloride catalyzes the cross-linking during the polymerization process because the two positive charges on the magnesium ion can make two bonds with two oxygen (carboxyl in KPA) [38]. Furthermore, the new peaks at 690, 592, and 420 cm^{-1} can be ascribed to the Mg–O stretching vibration [39].

Figure 6 describes the FTIR spectra of PVA as well as the Mg-PVA (0.55 g of $MgCl_2$) SAP. The main peaks of PVA were observed at 3,392, 2,922, 1,599, 1,413, and 1,101 cm^{-1}. These peaks are ascribed to the O–H stretching vibration of the hydroxyl group, asymmetric stretching vibration of C–H, C–C stretching vibration, bending vibration of $–CH_2$, and stretching vibration of C–O, respectively. Mg-PVA had similar peaks and two additional peaks attributable to Mg–O stretching vibrations at 860 and 692 cm^{-1} [40,41].

5.2 UV-Vis spectroscopy

UV-Vis spectroscopy gives valuable information on polymeric materials' reflectance, absorbance, and transmittance [42]. It is well known that PVA and KPA are essential polymers because they have excellent optical properties, such as great translucency. The UV-Vis absorbance spectra of KPA and Mg-PA (0.6 g of $MgCl_2$), and PVA and Mg-PVA (0.55 g of $MgCl_2$) dispersion are depicted in Figures 7 and 8, respectively. The absorbance spectra of KPA and PVA show a distinct peak at 260 nm, attributed to the carbonyl in the carboxylic group and n–π* in KPA and PVA. Both KPA and PVA have an absorption peak that increases to 261 nm with the addition of magnesium salt [43]. Mg-PVA SAP displays all the bands

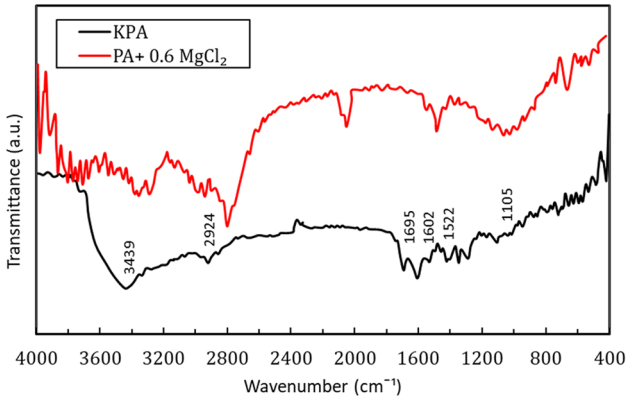

Figure 5: FTIR spectra of KPA and Mg-PA (0.6 g of $MgCl_2$).

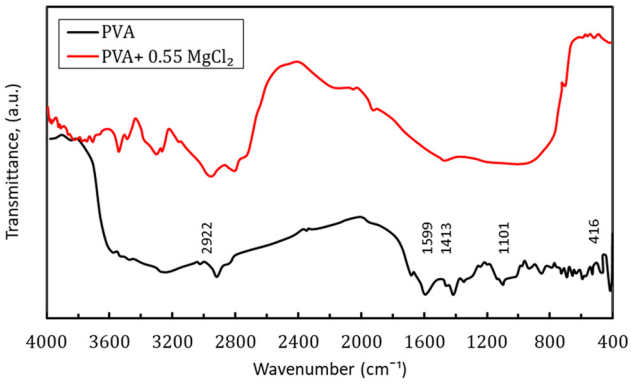

Figure 6: FTIR spectra of PVA and Mg-PVA (0.55 g of $MgCl_2$).

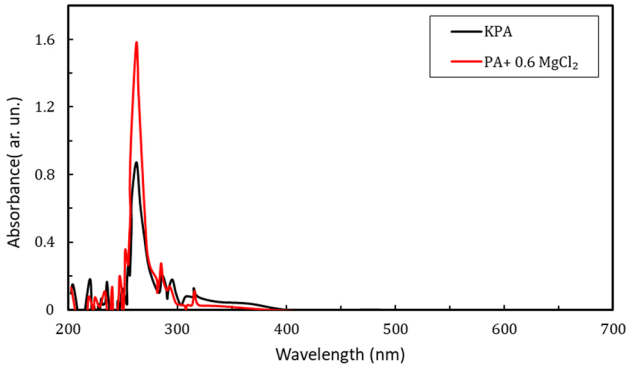

Figure 7: UV-Vis spectra of KPA and Mg-PA (0.6 g $MgCl_2$).

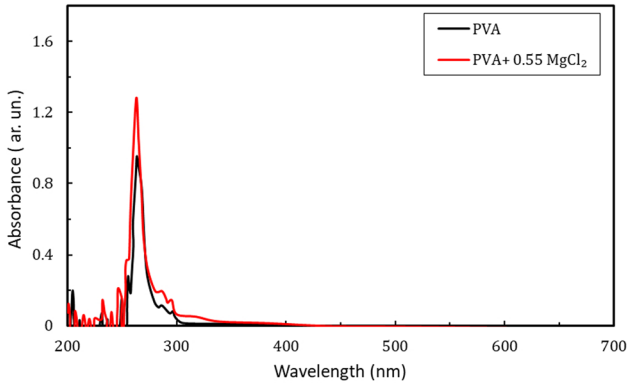

Figure 8: UV-Vis spectra of PVA and Mg-PVA (0.55 g $MgCl_2$).

spotted in neat PVA with a minor perversion inside the bands' location, and some of the bands disappear. Therefore, the UV-Vis spectra revealed that the absorption was mostly within the UV area, with a small visible wavelength range. This agrees with the study by researcher Deshmukh *et al.* who demonstrated that the UV spectra of polymer blends depending on cationic polyamine and anionic PVA [44].

5.3 SEM of SAPs

Figure 9a and b shows the KPA and Mg-PA SEM images. It can be noticed that KPA has a heterogeneous surface and a regular fibrous structure with agglomerates, which indicates that it is suitable for water absorption. Figure 9b shows the dispersion of the Mg^{2+} ions in the hydrogel composition. When $MgCl_2$ is present, it combines with KPA on its surface, forming an uneven fibrous structure [45,46]. The texture of the KPA and the Mg-PA containing 0.6 g $MgCl_2$ differed noticeably. These variations confirm the influence of the Mg^{2+} ions on the absorption of water molecules. We can say that the polymer structure has become similar to the structure of a porous sponge that can absorb more water.

The surface morphology of the PVA and Mg-PVA (0.55 g $MgCl_2$) SAPs got tested using SEM. According to Figure 9c and d, especially at low magnifications, PVA appears porous and has a porous structure, which becomes clearer at higher magnifications. The pores appear interconnected, overlapped, open-type, and uniformly scattered with nano or semi-macro dimensions [47]. A comparable microstructure is created when magnesium salts are added (Figure 9d), but it is less porous. Compared to structures without salts, the composition seems denser and less regular in its distribution of pores, and the pores appear more prominent. Magnesium salt acts as a catalyst, increasing the cross-linking rate during the polymerization process, creating a more cohesive molecular structure with a greater viscosity, generating structures with large pores and less distribution.

5.4 Influence of the cross-linker ($MgCl_2$) content on the water absorption capacity

Figure 10 shows the influence of the cross-linking material on the water absorption capacity. The water absorbency incremented when the $MgCl_2$ content increased from 0.4 to 0.6 g for KPA and from 0.33 to 0.55 g for PVA. When the content of $MgCl_2$ was 0.6 g for KPA and 0.55 g for PVA, the maximal absorbency was achieved at 650 and 244%, respectively. The three-dimensional networking created by the cross-links amid the polymer chains prevents the SAPs from dissolving in water, and the swelling process continues indefinitely. This effect is caused by the polymeric network's elastic retraction forces. The retraction forces balance and the chains tend to swell to indefinite dilution. Cross-linking happens most often during the polymerization reaction step of SAP manufacturing. SAP particles that have been cross-linked can considerably increase both flow and absorption pressure. During the swelling process, cross-linking agents protect the form of the particles. This results in a less tightly packed gel with air pockets, allowing the fluid to flow freely in high permeability patterns [48]. The first findings of the current lab investigation suggest that hydrogels could be used as water reservoirs in agriculture (Sánchez-Orozco *et al.*) [49]. In terms of hydrogel decomposition, current analyses reveal that it takes about

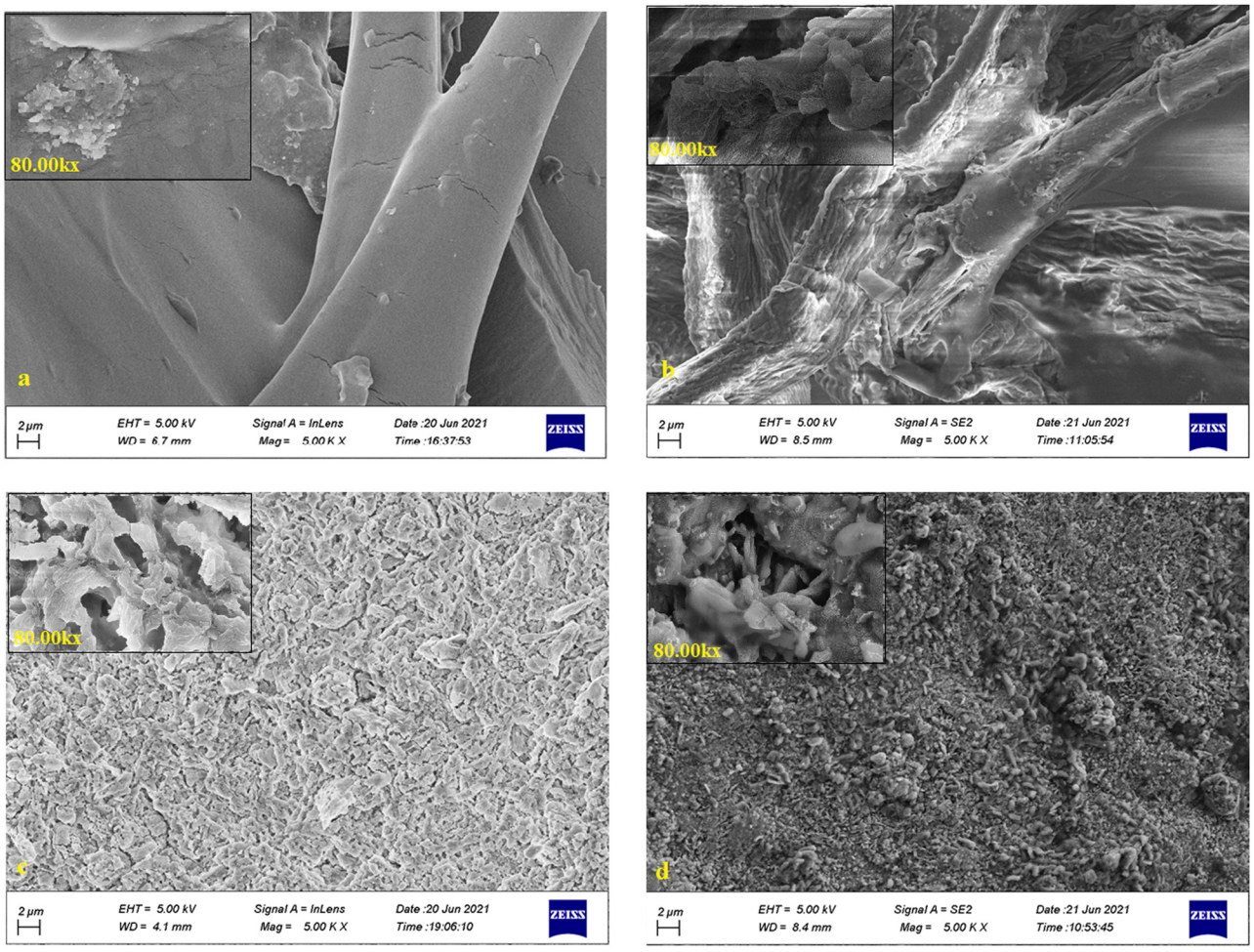

Figure 9: SEM image of (a) KPA, (b) Mg-PA (0.6 g $MgCl_2$), (c) PVA and (d) Mg-PVA (0.55 g $MgCl_2$).

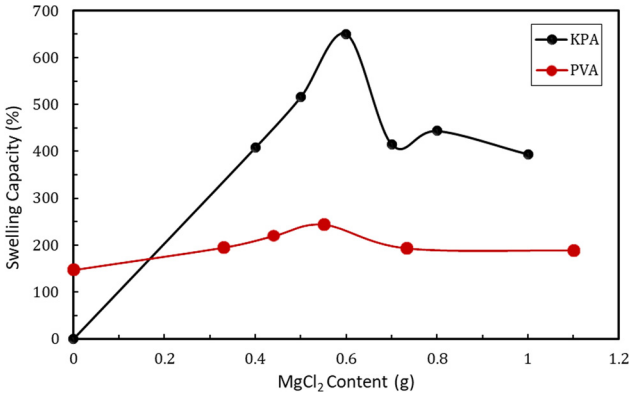

Figure 10: Effect of $MgCl_2$ content on swelling capacity.

6 months (Gubisová *et al.*) for the hydrogel to degrade, with no major changes in soil chemistry [50]. However, when the $MgCl_2$ content was above 0.6 g for KPA and above 0.55 g for PVA, the SAP was more rigid because of the excessive cross-linker. It could not absorb more water, causing a denser network structure and poor water absorption [34].

5.5 Water retention

The water retaining ratio of SAPs was calculated, and the findings are shown in Figures 11 and 12. With time, the data showed a reduction in water retention. The graphs (Figures 11 and 12) show that Mg-PA SAP had a greater water retention equilibrium than Mg-PVA, which could only retain 73% of water after 12 h. Water retention might be caused by hydrogen bonds and Van der Waals forces amid water molecules and the SAPs [51]. The water retention capability of Mg-PA increases with the increase in $MgCl_2$. At room temperature and after 12 h, the water retaining ratios of KPA at 1, 0.8, 0.7, 0.6, 0.5, and 0.4 g $MgCl_2$ were 73.05, 65.84, 70.67, 71.59, 50.03, and 55.48% respectively, and the water retention ratio of PVA at 1.1,

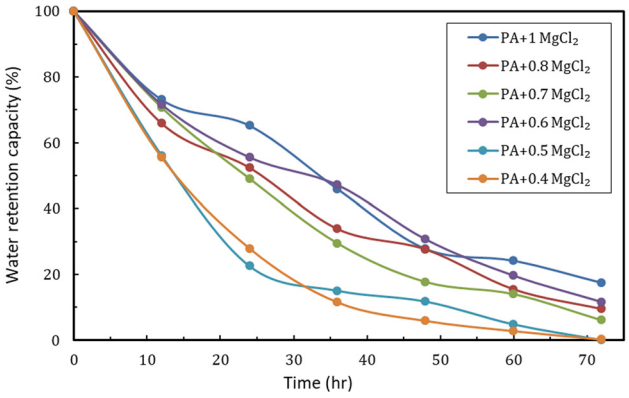

Figure 11: Water retention capacity (%) of KPA SAPs at various immersion times.

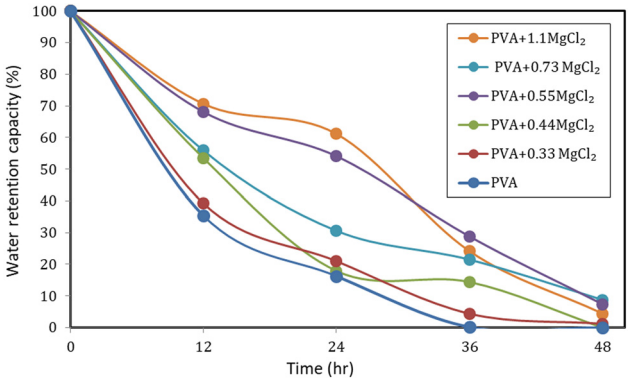

Figure 12: Water retention capacity (%) of PVA SAPs at various immersion times.

0.733, 0.55, 0.44, 0.33, and 0 g $MgCl_2$ were 70.65, 55.90, 68.10, 53.50, 39.24, and 35.39%, respectively. While SAPs had removed water after 48 h, the water retention ratios of KPA at 1, 0.8, 0.7, 0.6, 0.5, and 0.4 g $MgCl_2$ became 27.79, 27.66, 17.76, 30.71, 11.80, and 5.90%, respectively, and that of PVA became 4.46, 8.78, 7,40, 0, 1.22, and 0% for PVA at 1.1, 0.733, 0.55, 0.44, 0.33, and 0 g $MgCl_2$, respectively. The network structure of KPA SAP is more compact than that of PVA SAP, and the robust network structure is responsible for better water retention ability. Simultaneously, increased water absorption capacity can help with water retention [52].

5.6 TGA

A thermal degradation investigation [53] is a good predictor of a superabsorbent material's capacity to withstand high-temperature circumstances. As a result, TG curves of KPA, Mg-PA (0.6 g $MgCl_2$), PVA, and Mg-PVA (0.55 g $MgCl_2$) were produced using their dry, primary weights of 8.725, 4.660, 7.242, and 1.753 mg, respectively (Figure 13). The weight loss curves of KPA and PVA were greater than those of Mg-PA and Mg-PVA at temperatures below 100°C, respectively. The KPA sample's weight loss curve revealed three phases of heat decomposition. The loss of bound water adsorbed on the surface of the particles represents the first phase of decomposition. Intermolecular dehydration reacting and several primary decomposition processes are involved in the second phase of decomposition. The third phase of decomposition of the KPA and PVA is attributed to decomposition reactions between 370–410°C and 175–250°C, respectively. All stages of decomposition are listed in Table 1.

5.7 DSC analysis

DSC represents a thermal analyzing procedure where the heat that flows in or out of a specimen can be measured as temperature or time [54]. Figure 14(a) displays the DSC curves of the KPA. An endothermic step change (30–45°C) occurs first in the scan, followed by an exothermic peak (45–60°C). Then, endothermic curve occurs between 60 and 100°C, and after that exothermic curve occurs between 100 and 352.01°C. This effect is due to the dissociation of water molecules. The third endothermic effect occurs between 352.01 and 374.87°C, which is caused by the decomposition of KPA material. An exothermic step occurs above 374.87°C due to the release of heat formation of the material.

An endothermic peak of Mg-PA (0.6 g of $MgCl_2$) changed (30–45°C) and occurred first in the scan, followed by an exothermic peak (45–72.06°C), which is then followed by the endothermic peak (72.06–92.95°C). This effect is due to the dissociation of water molecules. The second endothermic effect occurs between (243.73–273.7°C), which is higher than the first step. This process is due to the decomposition of the Mg-PA compound. Finally, an exothermic step occurs above 273.7°C due to the release of heat formation of compound species. These results are shown in Figure 14(b).

Figure 14(c) and (d) displays the DSC curves of PVA and PVA-Mg (0.55 g $MgCl_2$). The endothermic peak of PVA and Mg-PVA changed (30–45°C) and occurred first in the scan, followed by an exothermic peak (45–213.97°C) for PVA and (45–220.52°C) for Mg-PVA, this effect was due to the evaporation of water molecules. This is followed

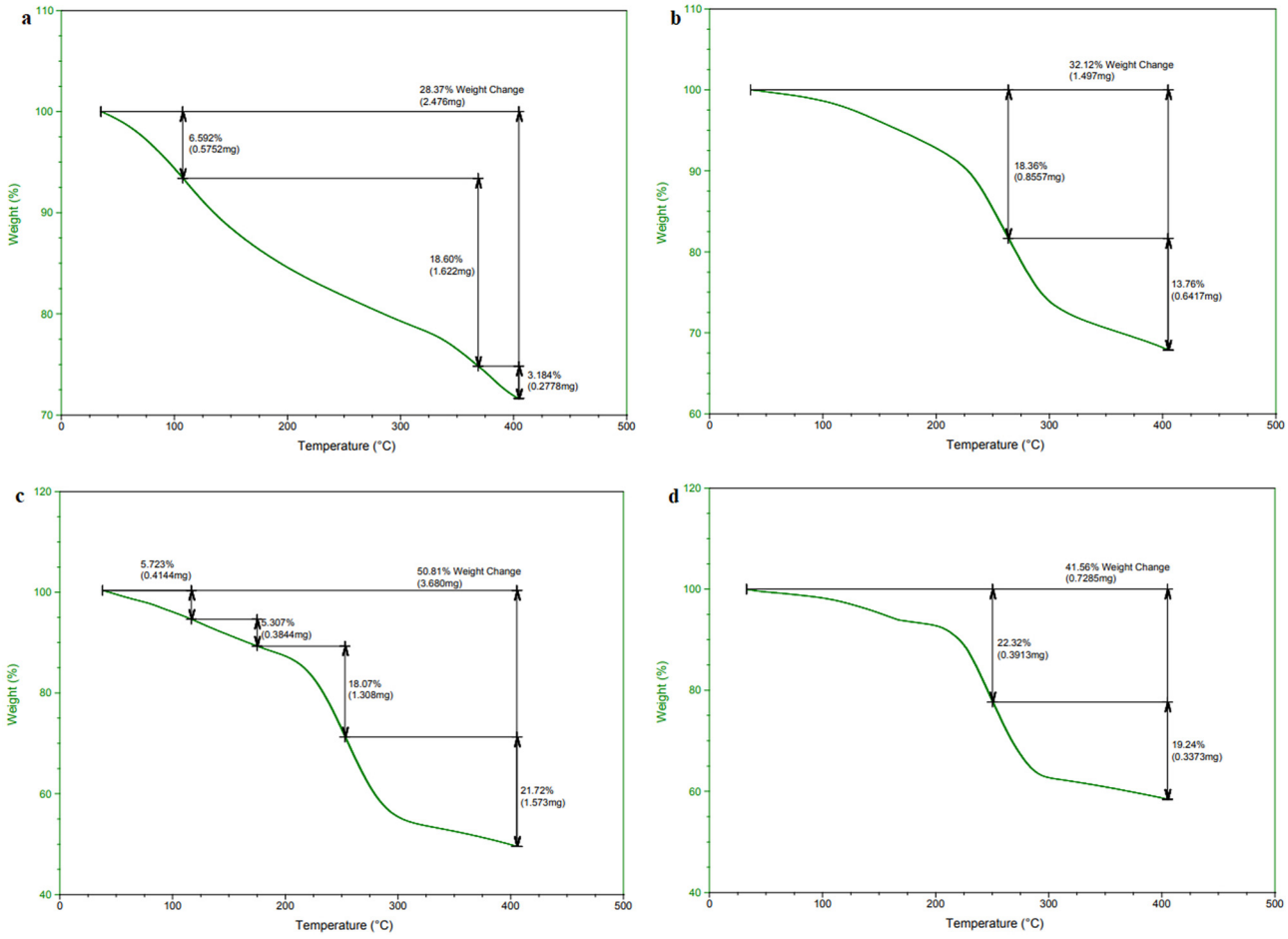

Figure 13: TGA spectra of (a) KPA, (b) Mg-PA, (c) PVA, and (d) Mg-PVA with their indicated weight losses.

Table 1: Mass loss of KPA, Mg-PA, PVA, and Mg-PVA at various temperatures

Polymer	T_{start} (°C)	T_{end} (°C)	Total mass loss (%)	Total mass loss (mg)	Mass loss step (%)	Mass loss step (mg)
KPA	30	105	6.59	0.6	6.6	0.6
	105	370	25.19	2.2	18.6	1.6
	370	410	28.38	2.5	3.2	0.3
Mg-PA	30	260	6.59	0.6	18.4	0.9
	260	410	20.35	1.8	13.8	0.6
PVA	30	115	6.59	0.6	5.7	0.4
	115	175	11.90	1.0	5.3	0.4
	175	250	29.97	2.6	18.1	1.3
	250	400	51.69	4.5	21.7	1.6
Mg-PVA	30	250	6.59	0.6	22.3	0.4
	250	400	25.83	2.3	19.2	0.3

by the endothermic effect between 213.97 and 263.65°C for PVA and between 220.52 and 261.24°C for Mg-PVA. Finally, an exothermic step occurs above 263.65°C for PVA and above 261.24°C for Mg-PVA, due to the release of heat formed in the compound species.

6 Conclusion

SAPs were successfully produced by the solution polymerization of KPA or PVA with magnesium salt to form the SAPs Mg-PA and Mg-PVA, respectively. Mg-PA (0.6 g $MgCl_2$) had a water absorbency of 650%, while Mg-PVA (0.55 g $MgCl_2$) had a water absorbency of 244%. According to FTIR, UV-Vis spectroscopy, SEM, TGA, and DSC results, the SAPs (Mg-PA and Mg-PVA) were prepared successfully. Mg-PA SAP has superior water absorption and water retention capability than Mg-PVA SAP in distilled water. The water retaining capability of the polymer increased with the increase in the magnesium salt $MgCl_2$. Finally, the findings of this study support the use of PA-Mg as a superabsorbent material in agricultural areas to keep soil moisture as long as possible, and thus eliminate the need for frequent water spraying.

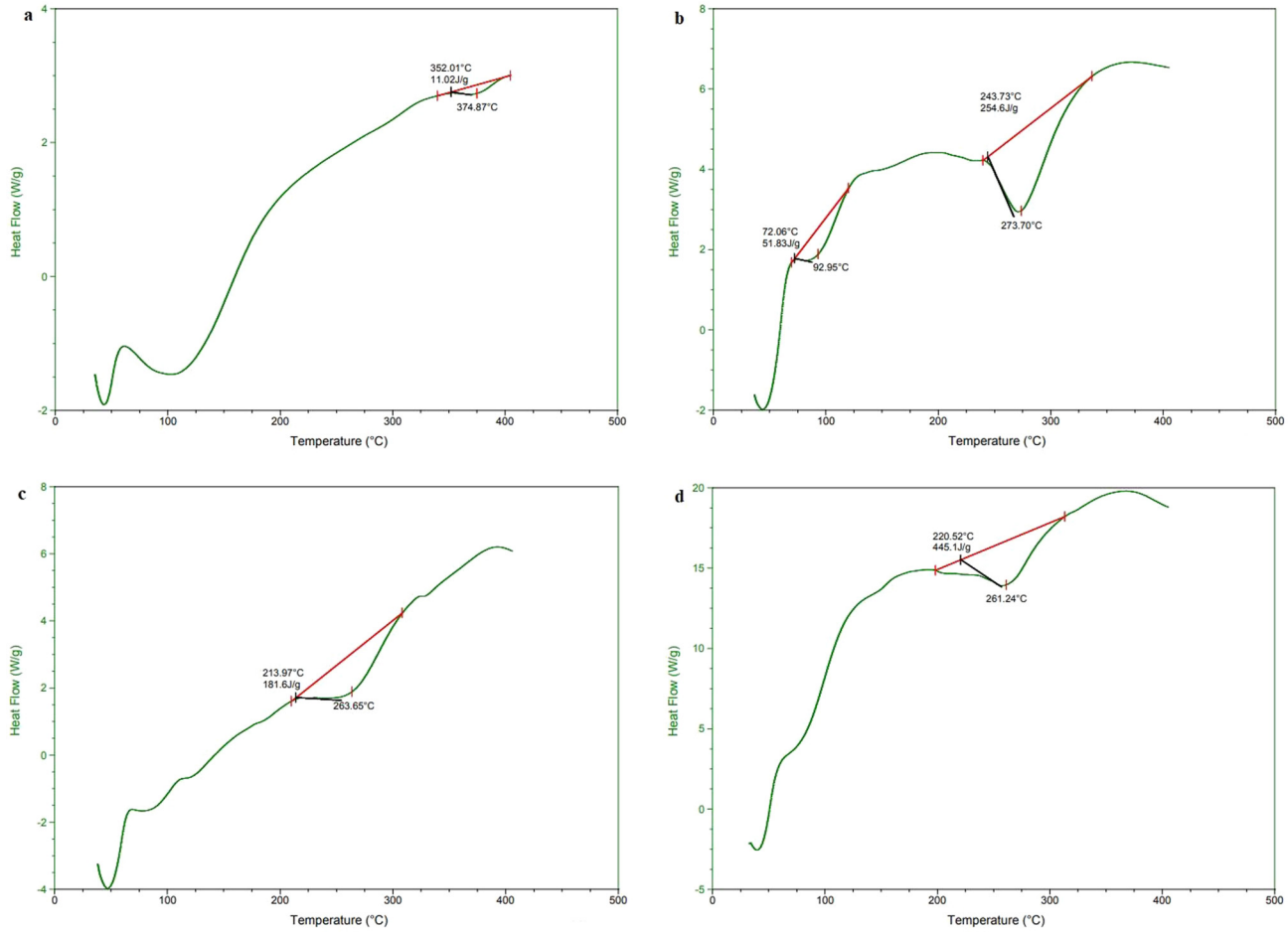

Figure 14: Differential scanning calorimetry analysis of (a) KPA, (b) Mg-PA (0.6 g $MgCl_2$), (c) PVA, and (d) Mg-PVA (0.55 g $MgCl_2$).

Acknowledgment: The authors express their appreciation to Senior Researcher Ali J. Addie and our appreciation to all staff of the Journal.

Funding information: The authors state no funding involved.

Author contributions: All authors have accepted responsibility for the entire content of this manuscript and approved its submission.

Conflict of interest: Authors state no conflict of interest.

References

[1] Buchholz FL, Graham AT. Modern superabsorbent polymer technology. New York: Wiley-VCH; 1998. [chapters 1–7].

[2] Ahmed AH, Hamdoon AM, Riaz AK, Varsha S, Abdellatif B, Mohammad Y, et al. Nano-scale delivery: A comprehensive review of nano-structured devices, preparative techniques, site-specificity designs, biomedical applications, commercial products, and references to safety, cellular uptake, and organ toxicity. J Mech Behav Mater. 2021;10:1493–559.

[3] Khattab MM, Tobeia SB, Jessam LM. The effects of different polymer materials on concrete properties containing super-absorbent polymers (SAP)-experimental study. IOP Conf Ser: Mater Sci Eng. 2020;737(1):012053.

[4] Ahmed EM. Hydrogel: preparation, characterization, and applications: a review. J Adv Res. 2015;6(2):105–21.

[5] Bukhari SMH, Khan S, Rehanullah M, Ranjha NM. Synthesis and characterization of chemically cross-linked acrylic acid/gelatin hydrogels: effect of pH and composition on swelling and drug release. Int J Polym Sci. 2015;2015:15–5. doi: 10.1155/2015/187961.

[6] Souza AJ, Guimarães RJ, Dominghetti AW, Scalco MS, Rezende TT. Water-retaining polymer and seedling type when planting irrigated coffee. Rev Ciênc Agron. 2016;47:334–43.

[7] Thombare N, Mishra S, Siddiqui MZ, Jha U, Singh D, Mahajan GR. Design and development of guar gum based novel, superabsorbent and moisture retaining hydrogels for agricultural applications. Carbohydr Polym. 2018;185:169–78.

[8] Zhang L, Li K, Xiao W, Zheng L, Xiao Y, Fan H. Preparation of collagen–chondroitin sulfate–hyaluronic acid hybrid hydrogel

scaffolds and cell compatibility *in vitro*. Carbohydr Polym. 2011;84(1):118–25.
[9] Saul JM, Williams DF. Hydrogels in regenerative. In: Modjarrad K, Ebnesajjad S, editors. Handbook of Polymer Applications in Medicine and Medical Devices. Norwich (NY), USA: William Andrew Publishing; 2011. p. 279–302. https://www.sciencedirect.com/science/article/pii/B9780323228053000128.
[10] Al-Hubboubi S, Al-Attar T, Al-Badry H, Abood S, Mohammed R, Haddhood B. Performance of super-absorbent polymer as an internal curing agent for self-compacting concrete. MATEC Web Conf. 2018;162:02023. doi: 10.1051/matecconf/201816202023.
[11] Yadav S, Madan J. Hydrogels: A review. Int J Pharm Life Sci. 2020;11(6):6711–7.
[12] Hamidi M, Azadi A, Rafiei P. Hydrogel nanoparticles in drug delivery. Adv Drug Deliv Rev. 2009;60(15):1638–49.
[13] Xiao X, Yu L, Xie F, Bao X, Liu H, Ji Z, et al. One-step method to prepare starch-based superabsorbent polymer for slow release of fertilizer. Chem Eng J. 2017;309:607–16.
[14] Xu L, Wang C, Cui Y, Li A, Qiao Y, Qiu D. Conjoined-network rendered stiff and tough hydrogel from biogenic molecules. Sci Adv. 2019;5:3442.
[15] Wei J, Yang H, Cao H, Tan T. Using polyaspartic acid hydro-gel as water retaining agent and its effect on plants under drought stress. Saudi J Biol Sci. 2016;23:654–9.
[16] Demitri C, Scalera F, Madaghiele M, Sannino A, Maffezzoli A. Potential of cellulose-based superabsorbent hydrogels as water reservoir in agriculture. Int J Polym Sci. 2013;2013:435073–6.
[17] Tsung H, Yang TH. Recent applications of polyacrylamide as biomaterials. Recent Pat Mater Sci. 2008;1:29–40.
[18] Chang L, Xu L, Liu Y, Qiu D. Superabsorbent polymers used for agricultural water retention. Polym Test. 2020;94:107021. doi: 10.1016/j.polymertesting.
[19] Valeria R, Rocío A, José L, Rivera A, Ana M, Roberto R. Synthesis and characterization of organogel from poly(acrylic acid) with cellulose acetate. J Mech Behav Mater. 2013;31:655–60.
[20] Ahmed AS, Mandal UK, Taher M, Susanti D, Jaffri JM. PVA-PEG physically cross-linked hydrogel film as a wound dressing: experimental design and optimization. Pharm Dev Technoly. 2018;23:751–60.
[21] Musa BH, Hameed NJ. Effect of crosslinking agent (glutaraldehyde) on the mechanical properties of (PVA/Starch) blend and (PVA/PEG) binary blend films. Phys Conf Ser. 2021;1795(1):012064. doi: 10.1088/1742-6596/1795/1/012064.
[22] Musa BH, Hameed NJ. A study of the effect of starch content on the water absorption of PVA/Starch blends. Eng Technol J. 2021;39(1):150–8.
[23] Song Z, Liu J, Bai Y, Wei J, Li D, Wang Q, et al. Laboratory and field experiments on the effect of vinyl acetate polymer-reinforced soil. Appl Sci. 2019;9:208.
[24] Abbood B, Sukkar K, Al-Najar J. Characterization and Aerodynamics of Synthesized Polymeric Nanofibers via Electrospinning Process to Capture PM10 and PM2.5 from Air. J Appl Sci Nanotechnol. 2021;1(4):91–104.
[25] Xiong H-G, Tang S-W, Tang H-L, Zou P. The structure and properties of a starch-based biodegradable film. Carb Polym. 2008;71(2):263–8.
[26] Buthaina AI, Nahida JH, jáafr HK. Hydrogel and poly vinyl alcohol/chitosamine chloride blends preparation and study of their properties for medical uses. Eng Technol J. 2014;32(6 Part (B) Scientific):54–70.
[27] Elbarbary AM, El-Rehim HAA, El-Sawy NM, Hegazy ESA, Soliman ESA. Radiation-induced crosslinking of polyacrylamide incorporated low molecular weights natural polymers for possible use in the agricultural applications. Carbohydr Polym. 2017;08:050.
[28] Feng D, Bai B, Wang H, Suo Y. Novel Fabrication of PAA/PVA/Yeast superabsorbent with interpenetrating polymer network for ph-dependent selective adsorption of dyes. J Polym Env. 2018;26(2):567–88.
[29] Zhang M, Zhang S, Chen Z, Wang M, Cao J, Wang R. Preparation and characterization of superabsorbent polymers based on sawdust. Polymers (Basel). 2019:11;11.
[30] Aulia HR, Nasution DA, Wirjosentono B. Thermal and morphological properties of polyvinyl alcohol-based hydrogel containing microcrystal cellulose. Chem Sci Technol. 2020;1:312–8.
[31] Jafari M, Najafi GR, Sharif MA, Elyasi Z. Superabsorbent polymer composites derived from polyacrylic acid: Design and synthesis, characterization, and swelling capacities. Polym Polym Compos. 2021;29(6):733–9. doi: 10.1177/0967391120933482.
[32] Czarnecka E, Nowaczyk J. Synthesis and characterization superabsorbent polymers made of starch, acrylic acid, acrylamide, poly(Vinyl alcohol), 2 hydroxyethyl methacrylate, 2-acrylamido-2-methylpropane sulfonic acid. Int J Mol Sci. 2021;22(9).
[33] Sonker AK, Tiwari N, Nagarale RK, Verma V. Synergistic effect of cellulose nanowhiskers reinforcement and dicarboxylic acids crosslinking towards polyvinyl alcohol properties. J Polym Sci. 2016;54(16):2515–25.
[34] Shixin F, Guangjian W, Pengcheng LB, Ronge X, Song L, Yukun Q, et al. Synthesis of chitosan derivative graft acrylic acid superabsorbent polymers and its application as water retaining agent. Int J Biol Macromolecules. 2018;115:754–61.
[35] Tackett JE. Determination of Low Amounts of Carboxylate in Polyacrylamide Using FT-IR. Appl Spectrosc. 1990;44(9):158–1583.
[36] Juan Z, Puerto M, Sabino V. Effect of the sodium polyacrylate on the magnetite nanoparticles produced by green chemistry routes applicability in forward osmosis. Nanomaterials. 2018;8:470.
[37] Wan T, Huang R, Zhao Q, Xiong L, Qin L, Tan X, et al. Synthesis of wheat straw composite superabsorbent. J Appl Polym Sci. 2013;130(5):3404–10. doi: 10.1002/app.39573.
[38] Jones F, Farrow JB, van BW. An infrared study of a polyacrylate flocculant adsorbed on hematite. Langmuir. 1998;14(22):6512–7.
[39] Guo M, Muhammad F, Wang A, Qi W, Wang N, Guo Y, et al. Magnesium hydroxide nanoplates: a pH-responsive platform for hydrophobic anticancer drug delivery. J Mater Chem B. 2013;1(39):5273–8.
[40] Du W, Jiang L, Shi M, Yang Z, Zhang X. The modification mechanism and the effect of magnesium chloride on poly(vinyl alcohol) films. RSC Adv. 2019;9(3):1602–12.
[41] Polu AR, Kumar R, Rhee HW. Magnesium ion conducting solid polymer blend electrolyte based on biodegradable polymers and application in solid-state batteries. Ionics. 2015;21(1):125–32. doi: 10.1007/s11581-014-1174-4.

[42] Deshmukh SH, Burghate DK, Shilaska SN, Deshmukh PT. Optical properties of polyaniline doped PVC-PMMA thin films. Ind J Pure Appl Phys. 2008;46:344–8.
[43] Limpan N, Prodpran T, Benjakul S, Prasarpran S. Influences of degree of hydrolysis and molecular weight of poly(vinyl alcohol) (PVA) on properties of fish myofibrillar protein/PVA blend films. Food Hydrocoll. 2012;29:226–33.
[44] Deshmukh K, Ahmad J, Hagg MB. Fabrication and characterization of polymer blends consisting of cationic polyallylamine and anionic polyvinyl alcohol. Ionics. 2014;20:957–67.
[45] Qiao D, Liu H, Yu L, Bao X, Simon GP, Petinakis E, et al. Preparation and characterization of slow-release fertilizer encapsulated by starch-based superabsorbent polymer. Carbohydr Polym. 2016;147:146–54.
[46] Bortolin A, Aouada FA, Mattoso LHC, Ribeiro C. Nanocomposite PAAm/methyl cellulose/montmorillonite hydrogel: evidence of synergistic effects for the slow release of fertilizers. J Agric Food Chem. 2013;61(31):7431–9.
[47] Tu H, Yu Y, Chen JJ, Shi XW, Zhou JL, Deng HB, et al. Highly cost-effective and high-strength hydrogels as dye adsorbents from natural polymers: chitosan and cellulose. Polym Chem. 2017;19:2913–21.
[48] Alireza M, Gholam BM, Majid F, Hamedreza J. Synthesis of poly (acrylamide-co-itaconic acid)/MWCNTs superabsorbent hydrogel nanocomposite by ultrasound-assisted technique: Swelling behavior and Pb (II) adsorption capacity. Ultrason – Sonochem. 2018;49:1–12.
[49] Sánchez-Orozco R, Timoteo-Cruz B, Torres-Blancas T, Ureña-Núñez F. Valorization of superabsorbent polymers from used disposable diapers as soil moisture retainer. Int J Res –GRANTHAALAYAH. 2017;5(4):105–17.
[50] Gubišová M, Hudcovicová M, Matušinský P, Ondreičková K, Klčová L, Gubiš J. Superabsorbent polymer seed coating reduces leaching of fungicide but does not alter their effectiveness in suppressing pathogen infestation. Polymers (Basel). 2022;14(1):76.
[51] Wu F, Zhang Y, Liu L, Yao J. Synthesis and characterization of a novel cellulose-gpoly(acrylic acid-co-acrylamide) superabsorbent composite based on flax yarn waste. Carbohydr Polym. 2012;87(4):2519–25.
[52] Zhou Y, Fu S, Zhang L, Zhan H. Superabsorbent nanocomposite hydrogels made of carboxylated cellulose nanofibrils and CMC-g-p(AA-co-AM). Carbohydr Polym. 2013;97(2):429–35.
[53] Salehi MB, Asefe MM, Samira ZM. Polyacrylamide hydrogel application in sand control with compressive strength testing. Pet Sci. 2019;16(1):94–104.
[54] Jiang Z. Using DSC studying the relationship between water absorbency of superabsorbent polymer and its structure. IOP Conf Ser: Mater Sci Eng. 2020;774(1):012050.